

# Quasiclassical Theory on Third-Harmonic Generation in Conventional Superconductors with Paramagnetic Impurities

Takanobu Jujo \*

*Graduate School of Materials Science, Nara Institute of Science and Technology,  
Ikoma, Nara 630-0101, Japan*

(Received December 4, 2017)

We investigate the third-harmonic generation (THG) of  $s$ -wave superconductors under microwave pulse irradiation. We consider the effect of paramagnetic impurities on the THG intensity of dirty superconductors. The nonlinear response function is calculated using the method of the quasiclassical Green function. It is shown that the amplitude mode is included as the vertex correction and makes a predominant contribution to the THG intensity. When the effect of paramagnetic impurities is weak, the THG intensity shows a peak at the temperature at which the superconducting gap is about the same as the frequency of the incident pulse, similarly to in experiments. As the effect of paramagnetic impurities is strengthened, the peak of the THG intensity disappears. This indicates that time-reversal symmetry breaking due to paramagnetic impurities eliminates the well-defined amplitude mode. The result of our calculation shows that the existence of the amplitude mode can be confirmed through the THG intensity. The result of a semiquantitative calculation is in good agreement with the experimental result, and it also shows that the diamagnetic term is negligible.

## 1. Introduction

In recent years, studies on the nonlinear optical response in superconductors have advanced with the development of microwave spectroscopy. Many of these studies were on the dynamics of transient responses using pump-probe spectroscopy, and the main objective was to elucidate the interaction effect in superconductors including strongly correlated electron systems. (For a review, see Ref. 1 for example.)

Another important aspect of the nonlinear optical response in the research of superconductors is that we can investigate phenomena that do not appear in the linear response. The amplitude fluctuation of the superconducting order parameter<sup>2,3</sup> is a typical example because the amplitude mode is not reflected in the linear absorption

---

\*E-mail address: jujo@ms.aist-nara.ac.jp

spectrum. (This is different from the phenomenon that the phase mode is pushed up to a high energy by the long-range Coulomb interaction.<sup>4</sup>)

So far, the amplitude mode has been observed in the phonon spectrum through the coupling of the superconductivity and the charge density wave in a superconductor coexisting with the charge density wave state.<sup>5,6</sup> Recently, it has been reported that the amplitude mode can be observed in ordinary superconductors by pump-probe spectroscopy<sup>7</sup> and third-harmonic generation (THG).<sup>8</sup> The former experimental study asserted that the observed transient oscillation of optical conductivity is an expression of the amplitude mode. The latter showed that the peak appears at a temperature at which the superconducting gap is equal to the frequency of the incident wave. This may indicate the existence of the amplitude mode.<sup>9</sup>

Theoretically, the excitation of the amplitude mode overlaps the quasiparticle excitation by two-photon absorption in the spectrum.<sup>10</sup> Thus, it is required to distinguish these two phenomena in order to confirm the amplitude mode. As a proposal for identifying the amplitude mode, in this paper we investigate the THG intensity in superconductors with paramagnetic impurities. Time-reversal symmetry breaking due to paramagnetic impurities leads to instability of the amplitude mode.<sup>11</sup> Therefore, the peak of the THG intensity will decrease when the amplitude mode is dominant in the THG intensity. In addition, in order to clarify the existence of the amplitude mode, we conduct a semiquantitative evaluation, which has not been done so far (for example, supplementary materials of Refs. 8 and 12 and references therein), and compare it with the experimental result.

The following is the structure of this paper. Section 2 gives the formulation by the quasi-classical approximation for calculating the response function. Section 3 gives an expression for the THG intensity under pulse irradiation and shows the results of a numerical calculation such as its temperature dependence. A semiquantitative evaluation is also given. Section 4 gives an expression for the diamagnetic term and shows that this term is negligible in the THG intensity.

## 2. Formulation

A nonlinear current is written using the quasiclassical Green function ( $g^K$ ) as follows:<sup>13</sup>

$$J_\omega^\mu = e \int_{\text{FS}} v_k^\mu \frac{mk_F}{2\pi} \int \frac{d\epsilon}{4\pi i} \sum_{\nu=x,y,z} \text{Tr}[v_k^\nu \hat{g}_\nu^{K(3)}(\epsilon + \omega, \epsilon)]. \quad (1)$$

Here,  $v_k$  and  $m$  are the velocity and mass of electrons, respectively, and  $k_F$  is the Fermi wave number. (We put  $\hbar = c = 1$  in this paper with  $c$  the velocity of light.)  $\int_{\text{FS}}$  means integration on the Fermi surface. The superscripts  $K$  and (3) in  $\hat{g}^{K(3)}$  indicate the Keldysh Green function<sup>14</sup> and the third order of the external fields, respectively. The modifier “ $\hat{\phantom{x}}$ ” means a matrix in Nambu representation.  $\mu, \nu = x, y, z$  indicate spatial directions. We assume the isotropic case and omit this index hereafter.

$\hat{g}^{K(3)}(\epsilon + \omega, \epsilon)$  is derived from kinetic equations in the dirty limit.<sup>15,16</sup> In this limit the quasiclassical Green function can be divided into an odd order and an even order with respect to the external field. In the kinetic equation for the former, the effect of scattering by nonmagnetic impurities does not vanish in the collision integral and is predominant over other terms such as the superconducting gap. Thus, the kinetic equation in this case can be solved, and its solution is written as

$$\begin{aligned} \hat{g}^{K(3)}(\epsilon + \omega, \epsilon) = e \int \frac{d\omega'}{2\pi} A_{\omega'} \frac{-1}{2\alpha} & (\hat{g}_{\epsilon+\omega}^+ \hat{g}_{\epsilon+\omega-\omega',\epsilon}^K + \hat{g}_{\epsilon+\omega}^K \hat{g}_{\epsilon+\omega-\omega',\epsilon}^- + \hat{g}_{\epsilon,\epsilon-\omega+\omega'}^+ \hat{g}_{\epsilon-\omega}^K + \hat{g}_{\epsilon,\epsilon-\omega+\omega'}^K \hat{g}_{\epsilon-\omega}^- \\ & - \hat{\tau}_3 \hat{g}_{\epsilon}^+ \hat{\tau}_3 \hat{g}_{\epsilon,\epsilon-\omega+\omega'}^K - \hat{g}_{\epsilon}^K \hat{\tau}_3 \hat{g}_{\epsilon,\epsilon-\omega+\omega'}^- \hat{\tau}_3 - \hat{\tau}_3 \hat{g}_{\epsilon,\epsilon-\omega+\omega'}^+ \hat{\tau}_3 \hat{g}_{\epsilon-\omega+\omega'}^K - \hat{g}_{\epsilon,\epsilon-\omega+\omega'}^K \hat{\tau}_3 \hat{g}_{\epsilon-\omega+\omega'}^- \hat{\tau}_3). \end{aligned} \quad (2)$$

Here,  $\alpha = (mk_F/2\pi)n_i u_i^2$  with  $n_i$  the concentration of nonmagnetic impurities and  $u_i$  the magnitude of the potential. The dirty limit means that  $\alpha \gg \Delta$ .  $A_\omega$  is the external vector potential.  $\hat{\tau}_3 = \begin{pmatrix} 1 & 0 \\ 0 & -1 \end{pmatrix}$ .  $\hat{g}_\epsilon$  is the quasiclassical Green function in the equilibrium state and  $\hat{g}_{\epsilon,\epsilon'}$  is a second-order function on external fields (+ and - in the superscript indicate the retarded and advanced Green function, respectively). The kinetic equations for the latter are written as

$$\begin{aligned} \hat{\tau}_3 \epsilon \hat{g}_{\epsilon,\epsilon'}^+ - \hat{g}_{\epsilon,\epsilon'}^+ \epsilon' \hat{\tau}_3 - \left[ \hat{\tau}_3 \hat{\Sigma}_{\epsilon,\epsilon'}^+ \hat{g}_{\epsilon,\epsilon'}^+ - \hat{g}_{\epsilon,\epsilon'}^+ \hat{\Sigma}_{\epsilon'}^+ \hat{\tau}_3 + \hat{\tau}_3 \hat{\Sigma}_{\epsilon,\epsilon'}^+ \hat{g}_{\epsilon'}^+ - \hat{g}_{\epsilon'}^+ \hat{\Sigma}_{\epsilon,\epsilon'}^+ \hat{\tau}_3 \right] \\ - e^2 D_\alpha \int \frac{d\omega_1 d\omega_2}{(2\pi)^2} A_{\omega_1} A_{\omega_2} \left[ \hat{\tau}_3 \hat{g}_{\epsilon-\omega_1}^+ \hat{g}_{\epsilon'}^+ - \hat{g}_{\epsilon}^+ \hat{g}_{\epsilon'+\omega_1}^+ \hat{\tau}_3 \right] \delta(\epsilon - \epsilon' - \omega_1 - \omega_2) = 0 \end{aligned} \quad (3)$$

and

$$\begin{aligned} \hat{\tau}_3 \epsilon \hat{g}_{\epsilon,\epsilon'}^{(a)} - \hat{g}_{\epsilon,\epsilon'}^{(a)} \epsilon' \hat{\tau}_3 - \left[ \hat{\tau}_3 \hat{\Sigma}_{\epsilon,\epsilon'}^+ \hat{g}_{\epsilon,\epsilon'}^{(a)} - \hat{g}_{\epsilon,\epsilon'}^{(a)} \hat{\Sigma}_{\epsilon'}^- \hat{\tau}_3 + \hat{\tau}_3 \hat{\Sigma}_{\epsilon,\epsilon'}^{(a)} \hat{g}_{\epsilon'}^- - \hat{g}_{\epsilon'}^- \hat{\Sigma}_{\epsilon,\epsilon'}^{(a)} \hat{\tau}_3 \right] \\ - e^2 D_\alpha \int \frac{d\omega_1 d\omega_2}{(2\pi)^2} A_{\omega_1} A_{\omega_2} \left\{ \hat{\tau}_3 \left[ (t_{\epsilon-\omega_1}^h - t_{\epsilon-\omega_1-\omega_2}^h) \hat{g}_{\epsilon-\omega_1}^+ + (t_\epsilon^h - t_{\epsilon-\omega_1}^h) \hat{g}_{\epsilon-\omega_1}^- \right] \hat{g}_{\epsilon'}^- \right. \\ \left. - \hat{g}_{\epsilon'}^+ \left[ (t_{\epsilon'+\omega_1}^h - t_{\epsilon'}^h) \hat{g}_{\epsilon'+\omega_1}^+ + (t_{\epsilon'+\omega_1}^h - t_\epsilon^h) \hat{g}_{\epsilon'+\omega_1}^- \right] \hat{\tau}_3 \right\} \delta(\epsilon - \epsilon' - \omega_1 - \omega_2) = 0. \end{aligned} \quad (4)$$

Here,  $t_\epsilon^h := \tanh(\epsilon/2T)$  ( $T$  is temperature),  $\delta(\cdot)$  is the delta function, and  $\hat{g}_{\epsilon,\epsilon'}^{(a)} := \hat{g}_{\epsilon,\epsilon'}^K - t_{\epsilon'}^h \hat{g}_{\epsilon,\epsilon'}^+ + t_\epsilon^h \hat{g}_{\epsilon,\epsilon'}^-$  ( $\hat{g}^{(a)} = \hat{\Sigma}^{(a)} = \hat{0}$  in the equilibrium state).<sup>13</sup> The effect of impurity scatterings is calculated with the Born approximation,<sup>17</sup> and the interaction between

electrons and phonons is treated with the weak-coupling approximation. The self-energy is written as  $\hat{\Sigma}_{\epsilon,\epsilon'}^s = \hat{\Sigma}_{\epsilon,\epsilon'}^{(ep)s} + \hat{\Sigma}_{\epsilon,\epsilon'}^{(ni)s} + \hat{\Sigma}_{\epsilon,\epsilon'}^{(pi)s}$  with  $\hat{\Sigma}_{\epsilon,\epsilon'}^{(ni)s} = \alpha\hat{\tau}_3\hat{g}_{\epsilon,\epsilon'}^s\hat{\tau}_3$  (the effect of non-magnetic impurity scattering) and  $\hat{\Sigma}_{\epsilon,\epsilon'}^{(pi)s} = \alpha_p\hat{g}_{\epsilon,\epsilon'}^s$  (the effect of paramagnetic impurity scattering<sup>18,19</sup>) [ $s = +, -$  or  $(a)$ ].  $\hat{\Sigma}_{\epsilon,\epsilon'}^{(ep)+} = \hat{\Sigma}_{\epsilon,\epsilon'}^{(ep)-} = g_0 \int \frac{d\epsilon_1}{2\pi i} \hat{\tau}_3 \hat{g}_{\epsilon_1+(\epsilon-\epsilon')/2, \epsilon_1-(\epsilon-\epsilon')/2}^K \hat{\tau}_3$  (the electron–phonon interaction) and  $\hat{\Sigma}_{\epsilon,\epsilon'}^{(ep)(a)} = (t_\epsilon^h - t_{\epsilon'}^h) \hat{\Sigma}_{\epsilon,\epsilon'}^{(ep)+}$ .  $\alpha_p = (mk_F/2\pi)n'_i u'^2$  and  $g_0 = (mk_F/2\pi)(g_{ph}^2/\omega_D)$  with  $\omega_D$  the Debye frequency and  $g_{ph}$  the coupling constant between electrons and phonons.  $D_\alpha = v_F^2/6\alpha = v_F^2\tau/3$  ( $\tau = 1/2\alpha$  is the relaxation time) is the diffusion constant.

Equations (3) and (4) are solved by introducing

$$\hat{g}_{\epsilon,\epsilon'}^s = g_{\epsilon,\epsilon'}^s \hat{\tau}_0 + f_{\epsilon,\epsilon'}^s \hat{\tau}_1 \quad (5)$$

and

$$\hat{\Sigma}_{\epsilon,\epsilon'}^s = \Sigma_{\epsilon,\epsilon'}^{n,s} \hat{\tau}_0 + \Sigma_{\epsilon,\epsilon'}^{a,s} \hat{\tau}_1. \quad (6)$$

Here,  $n$  and  $a$  indicate the normal and anomalous self-energy, respectively.  $\hat{\tau}_0 = \begin{pmatrix} 1 & 0 \\ 0 & 1 \end{pmatrix}$  and  $\hat{\tau}_1 = \begin{pmatrix} 0 & 1 \\ 1 & 0 \end{pmatrix}$ .

By solving the above equations using  $\Sigma_\epsilon^{(ep)+} = \Sigma_\epsilon^{(ep)-} = \Delta\hat{\tau}_1$  ( $\Delta$  is the superconducting gap with the effect of impurity scattering included), the solution is written as

$$\begin{pmatrix} g_{\epsilon,\epsilon'}^s \\ f_{\epsilon,\epsilon'}^s \end{pmatrix} := e^2 D_\alpha \int \frac{d\omega_1 d\omega_2}{(2\pi)^2} A_{\omega_1} A_{\omega_2} \delta(\epsilon - \epsilon' - \omega_1 - \omega_2) \begin{pmatrix} \bar{g}_{\epsilon,\epsilon'}^s(\omega_1, \omega_2) \\ \bar{f}_{\epsilon,\epsilon'}^s(\omega_1, \omega_2) \end{pmatrix}. \quad (7)$$

Here,  $s = +, -, \text{ or } (a)$ , and

$$\begin{pmatrix} \bar{g}_{\epsilon,\epsilon'}^\pm(\omega_1, \omega_2) \\ \bar{f}_{\epsilon,\epsilon'}^\pm(\omega_1, \omega_2) \end{pmatrix} = \hat{M}_{\epsilon,\epsilon'}^{\pm\pm} \frac{1}{2} \left[ \begin{pmatrix} g_{\epsilon-\omega_1}^\pm \\ f_{\epsilon-\omega_1}^\pm \end{pmatrix} + \begin{pmatrix} g_{\epsilon-\omega_2}^\pm \\ f_{\epsilon-\omega_2}^\pm \end{pmatrix} \right] + \hat{M}_{\epsilon,\epsilon'}^{\pm\pm} \begin{pmatrix} 0 \\ \bar{\Sigma}_{\epsilon,\epsilon'}^{a,+}(\omega_1, \omega_2) \end{pmatrix} \quad (8)$$

(the double signs correspond), and

$$\begin{pmatrix} \bar{g}_{\epsilon,\epsilon'}^{(a)}(\omega_1, \omega_2) \\ \bar{f}_{\epsilon,\epsilon'}^{(a)}(\omega_1, \omega_2) \end{pmatrix} = \hat{M}_{\epsilon,\epsilon'}^{+-} \frac{1}{2} \sum_{\omega'=\omega_1, \omega_2} \left[ (t_{\epsilon-\omega'}^h - t_{\epsilon'}^h) \begin{pmatrix} g_{\epsilon-\omega'}^+ \\ f_{\epsilon-\omega'}^+ \end{pmatrix} + (t_\epsilon^h - t_{\epsilon-\omega'}^h) \begin{pmatrix} g_{\epsilon-\omega'}^- \\ f_{\epsilon-\omega'}^- \end{pmatrix} \right] \\ + \hat{M}_{\epsilon,\epsilon'}^{+-} (t_\epsilon^h - t_{\epsilon'}^h) \begin{pmatrix} 0 \\ \bar{\Sigma}_{\epsilon,\epsilon'}^{a,+}(\omega_1, \omega_2) \end{pmatrix}. \quad (9)$$

Here,  $\bar{\Sigma}$  indicates the vertex correction, which is calculated in the next subsection, and the diagonal element ( $\bar{\Sigma}^{n,+}$ ) is shown to vanish.

$$\hat{M}_{\epsilon,\epsilon'}^{ab} := \frac{i [\hat{\tau}_3 - X_{\epsilon,\epsilon'}^{ab} \hat{\tau}_0 - Y_{\epsilon,\epsilon'}^{ab} \hat{\tau}_1]}{z_\epsilon^a + z_{\epsilon'}^b + 2i\alpha_p X_{\epsilon,\epsilon'}^{ab}}. \quad (10)$$

Here,  $X_{\epsilon,\epsilon'}^{ab} := (\epsilon_p^a \epsilon_p'^b + \Delta_\epsilon^a \Delta_{\epsilon'}^b) / z_\epsilon^a z_{\epsilon'}^b$ ,  $Y_{\epsilon,\epsilon'}^{ab} := (\epsilon_p^a \Delta_{\epsilon'}^b + \Delta_\epsilon^a \epsilon_p'^b) / z_\epsilon^a z_{\epsilon'}^b$ ,  $\epsilon_p^\pm := \epsilon - \alpha_p g_\epsilon^\pm$ ,  $\Delta_\epsilon^\pm := \Delta + \alpha_p f_\epsilon^\pm$ , and  $z_\epsilon^\pm := \sqrt{(\epsilon_p^\pm)^2 - (\Delta_\epsilon^\pm)^2}$ . Quasiclassical Green functions in the equilibrium state are written as  $g_\epsilon^\pm = -i\epsilon_p^\pm / z_\epsilon^\pm$  and  $f_\epsilon^\pm = -i\Delta_\epsilon^\pm / z_\epsilon^\pm$ .

By using the above results, the nonlinear current is written as

$$J_\omega = - (e^2 D_\alpha)^2 \frac{mk_F}{2\pi} \int \frac{dw dw'}{(2\pi)^3} A_{\omega-2w} A_{\omega+w'/2} A_{\omega-w'/2} I_{\omega,w,w'}^{(3)}. \quad (11)$$

Here,

$$I_{\omega,w,w'}^{(3)} := \int \frac{d\epsilon}{4\pi i} \text{Tr} \left[ (\hat{g}_{\epsilon+\omega-w}^+ - \hat{\tau}_3 \hat{g}_{\epsilon+w}^+ \hat{\tau}_3 + \hat{g}_{\epsilon-\omega+w}^- - \hat{\tau}_3 \hat{g}_{\epsilon-w}^- \hat{\tau}_3) \hat{g}_{\epsilon+w,\epsilon-w(\omega+w'/2,w-w'/2)}^K \right. \\ \left. + (\hat{g}_{\epsilon+\omega-w}^K - \hat{\tau}_3 \hat{g}_{\epsilon+w}^K \hat{\tau}_3) \hat{g}_{\epsilon+w,\epsilon-w(\omega+w'/2,w-w'/2)}^- + (\hat{g}_{\epsilon-\omega+w}^K - \hat{\tau}_3 \hat{g}_{\epsilon-w}^K \hat{\tau}_3) \hat{g}_{\epsilon+w,\epsilon-w(\omega+w'/2,w-w'/2)}^+ \right]. \quad (12)$$

### 2.1 Vertex correction

We obtain  $\Sigma_{\epsilon,\epsilon'}^{(ep)+}$  by solving

$$\begin{pmatrix} \Sigma_{\epsilon,\epsilon'}^{(ep)n,+} \\ \Sigma_{\epsilon,\epsilon'}^{(ep)a,+} \end{pmatrix} = g_0 \int \frac{d\epsilon_1}{2\pi i} \hat{\tau}_3 \left[ \begin{pmatrix} g_{\epsilon_1+w,\epsilon_1-w}^{(a)} \\ f_{\epsilon_1+w,\epsilon_1-w}^{(a)} \end{pmatrix} + t_{\epsilon_1-w}^h \begin{pmatrix} g_{\epsilon_1+w,\epsilon_1-w}^+ \\ f_{\epsilon_1+w,\epsilon_1-w}^+ \end{pmatrix} - t_{\epsilon_1+w}^h \begin{pmatrix} g_{\epsilon_1+w,\epsilon_1-w}^- \\ f_{\epsilon_1+w,\epsilon_1-w}^- \end{pmatrix} \right] \quad (13)$$

$[w := (\epsilon - \epsilon')/2]$ . Using Eqs. (7)-(9) and

$$\begin{pmatrix} \Sigma_{\epsilon,\epsilon'}^{(ep)n,+} \\ \Sigma_{\epsilon,\epsilon'}^{(ep)a,+} \end{pmatrix} := e^2 D_\alpha \int \frac{d\omega_1 d\omega_2}{(2\pi)^2} A_{\omega_1} A_{\omega_2} \delta(\epsilon - \epsilon' - \omega_1 - \omega_2) \begin{pmatrix} \bar{\Sigma}_{\epsilon,\epsilon'(\omega_1,\omega_2)}^{n,+} \\ \bar{\Sigma}_{\epsilon,\epsilon'(\omega_1,\omega_2)}^{a,+} \end{pmatrix}, \quad (14)$$

the solution is written as

$$\begin{pmatrix} \bar{\Sigma}_{\epsilon,\epsilon'(\omega_1,\omega_2)}^{n,+} \\ \bar{\Sigma}_{\epsilon,\epsilon'(\omega_1,\omega_2)}^{a,+} \end{pmatrix} = \frac{g_0}{2D_{2w}} \int \frac{d\epsilon_1}{2\pi i} \begin{pmatrix} 0 & 0 \\ 0 & -1 \end{pmatrix} \sum_{s,s'=\pm} s \left[ (t_{\epsilon_1-s'w'}^h - t_{\epsilon_1-sw}^h) \hat{M}_{\epsilon_1+w,\epsilon_1-w}^{+-} \right. \\ \left. + t_{\epsilon_1-sw}^h \hat{M}_{\epsilon_1+w,\epsilon_1-w}^{ss} \right] \begin{pmatrix} g_{\epsilon_1-s'w'}^s \\ f_{\epsilon_1-s'w'}^s \end{pmatrix} \quad (15)$$

with  $w = \epsilon - \epsilon' = (\omega_1 + \omega_2)/2$  and  $w' = (\omega_1 - \omega_2)/2$ . Here,

$$D_{2w} = 1 - g_0 \int \frac{d\epsilon_1}{2\pi i} \left[ (t_{\epsilon_1+w}^h - t_{\epsilon_1-w}^h) m_{\epsilon_1+w,\epsilon_1-w}^{+-} + t_{\epsilon_1-w}^h m_{\epsilon_1+w,\epsilon_1-w}^{++} - t_{\epsilon_1+w}^h m_{\epsilon_1+w,\epsilon_1-w}^{--} \right] \quad (16)$$

with

$$m_{\epsilon,\epsilon'}^{ab} := \frac{i(1 + X_{\epsilon,\epsilon'}^{ab})}{z_\epsilon^a + z_{\epsilon'}^b + 2i\alpha_p X_{\epsilon,\epsilon'}^{ab}}. \quad (17)$$

### 3. Third-Harmonic Generation

#### 3.1 Nonlinear response under incident pulse

The electric field is written as  $\tilde{E}_t = \bar{E}_t e^{-i\Omega t} + \bar{E}_t^* e^{i\Omega t}$ . Using of this field, the vector potential is written as  $A_\omega = E_\omega/i\omega$  with  $E_\omega = \int \frac{dt}{2\pi} \tilde{E}_t e^{i\omega t}$ . We assume a Gaussian pulse for  $\bar{E}_t$ :  $|\bar{E}_t| = \bar{E}_0 e^{-(t/t_0)^2}$ . Then

$$A_\omega = \frac{\sqrt{\pi}t_0}{i\omega} \left[ \bar{E}_0 e^{-(\omega-\Omega)^2/4c} + \bar{E}_0^* e^{-(\omega+\Omega)^2/4c} \right],$$

and we introduce a dimensionless external field,

$$\bar{A}_\omega := \frac{\Delta_0}{\sqrt{\pi}t_0|\bar{E}_0|} A_\omega.$$

( $\Delta_0$  is the superconducting gap at  $T = 0$  without impurity scatterings.) Using of  $\bar{A}_\omega$ , the current [Eq. (11)] is rewritten as

$$J_\omega = \sigma_0 |E_\Omega| \left( \frac{e|\bar{E}_0|\xi_0}{\Delta_0} \right)^2 \frac{l}{\xi_0} j_\omega \quad (18)$$

with

$$j_\omega := \frac{-1}{48} \int dw dw' t_0^2 \bar{A}_{\omega-2w} \bar{A}_{\omega+w'/2} \bar{A}_{\omega-w'/2} I_{\omega,w,w'}^{(3)}. \quad (19)$$

Here,  $|E_\Omega| = \sqrt{\pi}t_0|\bar{E}_0 + \bar{E}_0^* e^{-(\Omega t_0)^2}| \simeq \sqrt{\pi}t_0|\bar{E}_0|$  and  $\sigma_0 = n_e e^2 \tau / m = e^2 D_\alpha m k_F / \pi^2$  are used.  $\xi_0 = v_F / \pi \Delta_0$  and  $l = v_F \tau$  are the coherence length and the mean free path, respectively.

Equation (12) does not depend on  $\alpha$ . This is because  $\hat{g}_\epsilon^s$  and  $\hat{g}_{\epsilon,\epsilon'}^s$  do not include  $\alpha$  owing to Anderson's theorem<sup>20</sup> and the absence of a collision term derived from nonmagnetic impurity scattering,<sup>21,22</sup> respectively. The dependence of the nonlinear current [Eq. (18)] on nonmagnetic impurity scattering is included only in  $l$ . Thus, the following numerical calculations are performed without specifying the value of  $\alpha$ .

#### 3.2 Numerical calculations

We calculate the THG intensity using the dimensionless  $j_\omega$  from Eq. (19). We take  $\Delta_0$  as the unit of energy ( $\Delta_0 = 1$ ), and in the variables in the subsequent figures, the notation of  $\Delta_0$  is omitted for the sake of simplicity.

The dependence of the THG intensity ( $|j_{3\Omega}|^2$  with  $\Omega$  the frequency of the incident pulse) on temperature is shown in Fig. 1. There is a sharp peak for small values of  $\alpha_p$ . This peak becomes blurred and shifts to low temperatures with increasing  $\alpha_p$ . As shown below, this behavior is caused by the fact that this peak originates from the amplitude mode, and the blurring occurs owing to the vanishing of the well-defined mode for finite

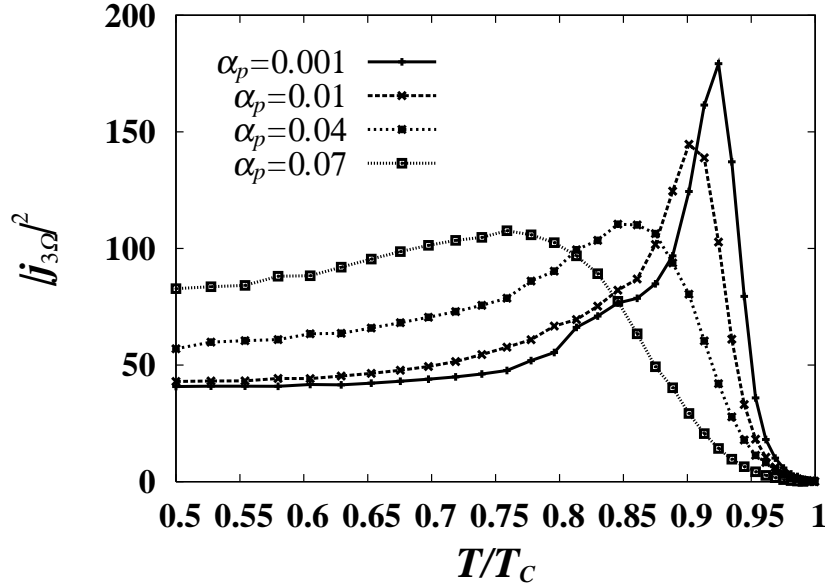


**Fig. 1.** Dependence of the dimensionless THG intensity  $|j_{3\Omega}|^2$  on temperature ( $T$  normalized by the transition temperature  $T_C$ ) for various values of  $\alpha_p$  (the effect of paramagnetic impurities).  $\Omega = 0.46\Delta_0$  (the frequency of the incident pulse).  $1/t_0^2 = 0.003\Delta_0^2$ . (This value corresponds to the full width at half maximum  $\delta\Omega = 4\sqrt{\ln 2}/t_0 \simeq 0.18\Delta_0$ .)

values of  $\alpha_p$ .

The amplitude mode described by  $D_{2\omega}$  [Eq. (16)] is included in the vertex correction  $\bar{\Sigma}^a$  [Eq. (15)]. The THG intensities with and without the vertex correction are shown in Figs. 2(a) and 2(b), respectively. Figure 2(a) [2(b)] is calculated using  $\bar{g}_\omega$ , in which only the second [first] terms in the left-hand side of Eqs. (8) and (9) are included. The THG intensity is proportional to the square of the absolute value of  $j_{3\Omega}$ , and thus, the result in Fig. 1 is not a simple summation of the results in Figs. 2(a) and 2(b). Figure 2(a) indicates that the vertex correction causes a sharp peak for small values of  $\alpha_p$ .

The dependence of the amplitude mode ( $D_{2\omega}$ ) on the frequency  $\omega$  at  $T/T_C = 0.5$  is shown in Fig. 3. Figure 3(a) shows that a well-defined amplitude mode disappears with increasing  $\alpha_p$ .  $-\text{Im}D_{2\omega}$  is the damping rate of the amplitude mode and takes finite values in the range  $\omega < \Delta$  for finite values of  $\alpha_p$ . This behavior originates from the fact that the gap edge ( $E_g$ ) of a one-particle spectrum is smaller than  $\Delta$  for finite values of  $\alpha_p$ :  $E_g = \Delta[1 - (2\alpha_p/\Delta)^{2/3}]^{3/2}$  (see Ref. 19).

We introduce  $\omega_{am}$  as the frequency at which  $\text{Re}D_{2\omega}$  takes a local minimum. The dependence of  $\omega_{am}$  on temperature is shown in Fig. 4. The values of  $\omega_{am}$  are numerically calculated from the dependences of  $\text{Re}D_{2\omega}$  on frequency. Figure 4 shows that  $\omega_{am} \simeq \Delta$

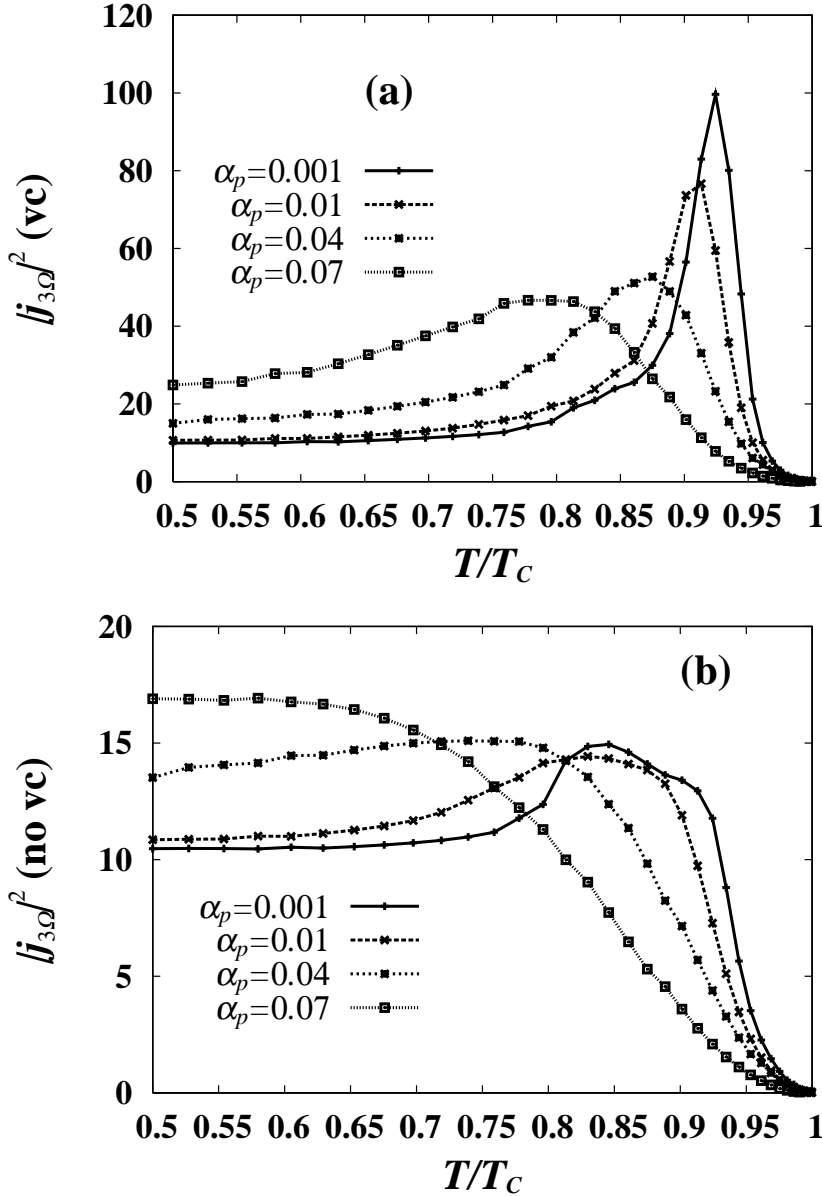


**Fig. 2.** (a) Temperature dependence of the THG intensity with only  $\bar{\Sigma}^a$  included. (b) Temperature dependence of the THG intensity without  $\bar{\Sigma}^a$ .  $\Omega = 0.46\Delta_0$  and  $1/t_0^2 = 0.003\Delta_0^2$ .

regardless of the value of  $\alpha_p$ . In contrast,  $E_g$  deviates from  $\Delta$  with increasing  $\alpha_p$  as noted above. The reason for including horizontal lines in Fig. 4 is to investigate how the peak of the THG intensity is related to the temperature at which the frequency ( $\Omega$ ) crosses  $\Delta$  or  $E_g$ .

The temperature (normalized by  $T_C$ ) at which  $\Delta$  (or  $E_g$ ) and  $\Omega$  ( $= 0.46\Delta_0, 0.69\Delta_0, 0.92\Delta_0$ ) intersect is shown in Fig. 5. ( $T_\Delta$  and  $T_{E_g}$  are dimensionless quantities.)  $T_\Delta$  and  $T_{E_g}$  are set to 0 when  $\Delta$  and  $E_g$  do not cross  $\Omega$ , respectively. Figures 1 and 5 show



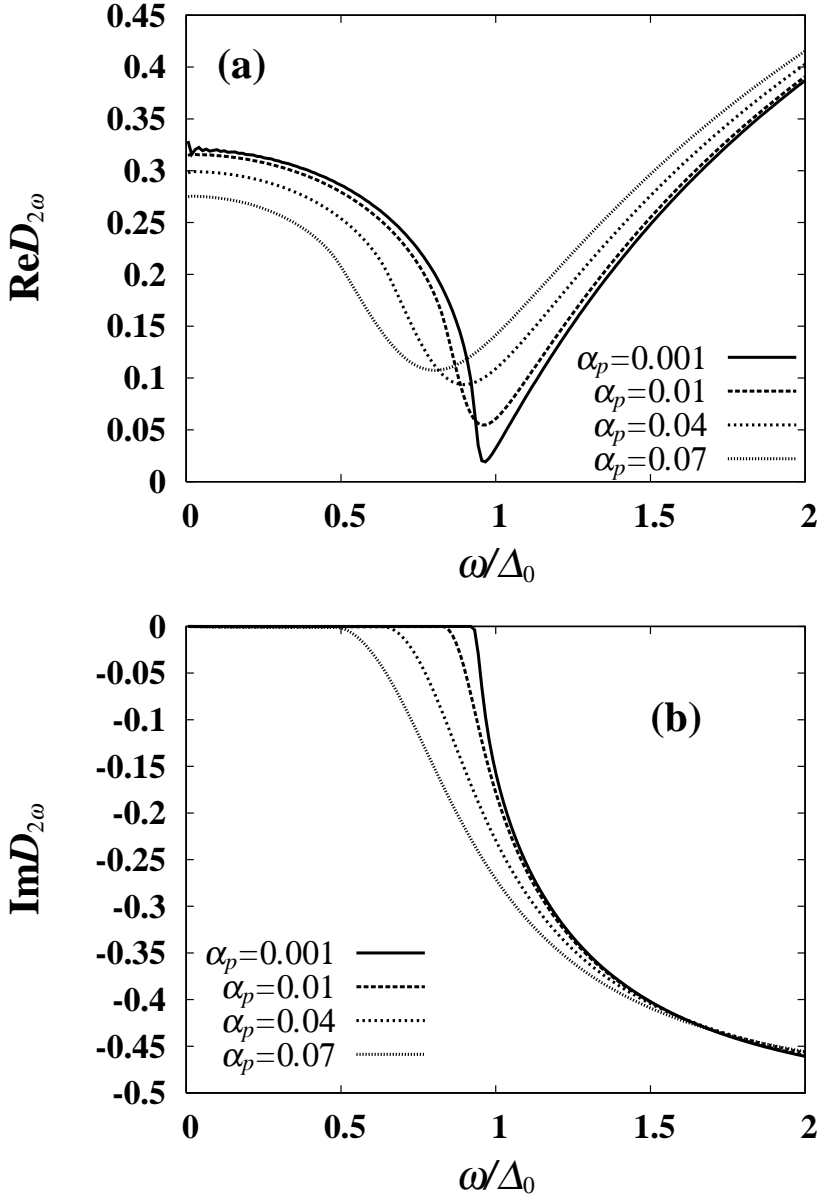


**Fig. 3.** (a) Frequency ( $\omega$ ) dependence of the real part of  $D_{2\omega}$  for various values of  $\alpha_p$ . (b) Frequency dependence of the imaginary part of  $D_{2\omega}$ .  $D_{2\omega}$  is a dimensionless quantity.  $T/T_C = 0.5$ .

that the THG intensity does not show a peak at  $T/T_C = T_\Delta$  or  $T/T_C = T_{E_g}$ . The temperature at which the THG intensity shows a peak is between  $T_\Delta$  and  $T_{E_g}$ .

This is verified by calculating the THG intensity for other values of  $\Omega$ . The THG intensities for  $\Omega = 0.69\Delta_0$  and  $\Omega = 0.92\Delta_0$  are shown in Figs. 6(a) and 6(b), respectively. Figures 6(a) and 6(b) show that the peak of the THG intensity almost vanishes in the case of  $T_{E_g} = 0$ . The deviation of the peak from  $T_\Delta$  is similar to the case of the two-photon absorption (TPA) spectrum. In the latter case, the frequency at which the

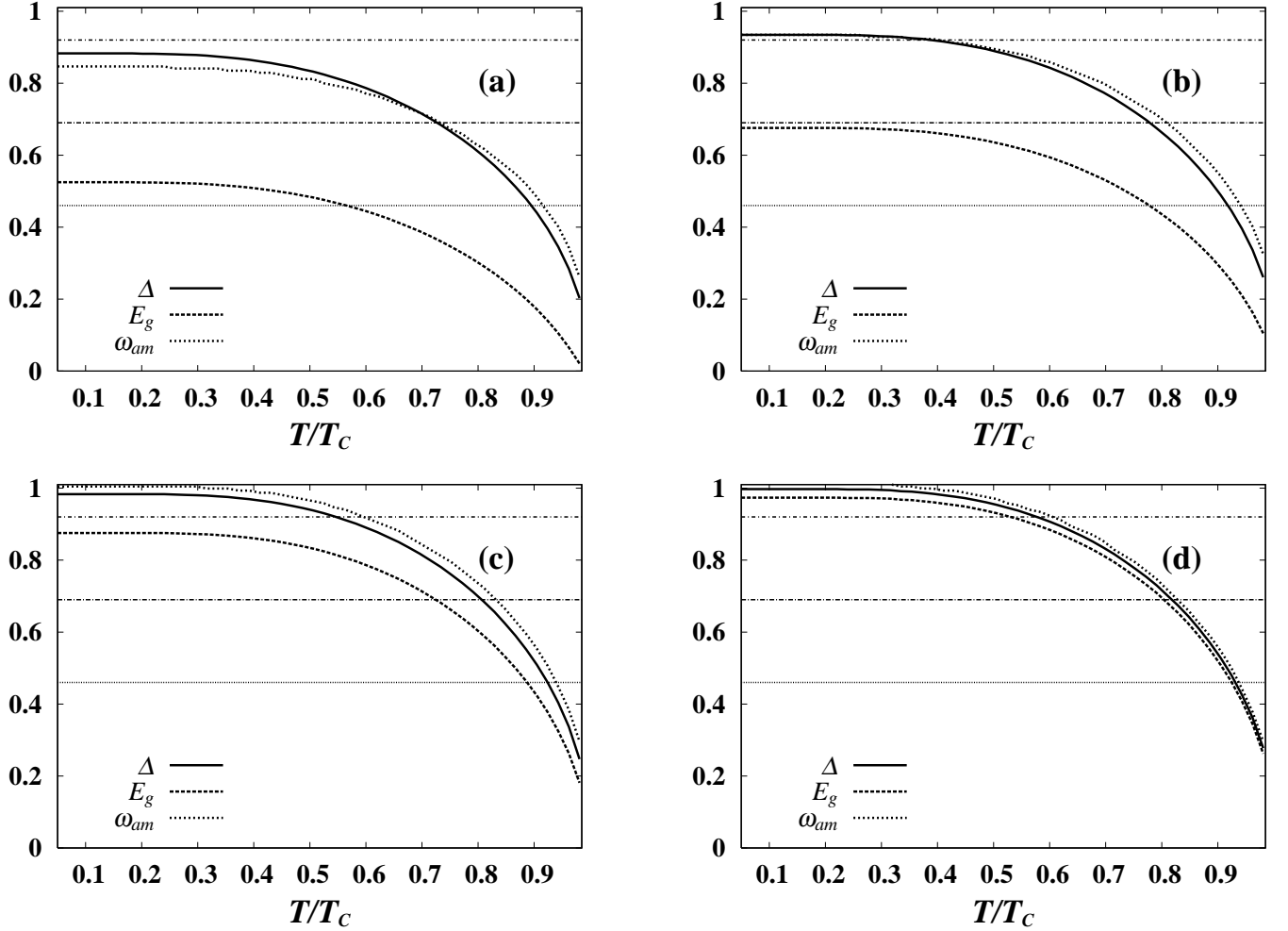


**Fig. 4.** Temperature dependences of  $\Delta$ ,  $E_g$ , and the frequency  $\omega_{am}$  (at which  $\text{Re}D_{2\omega}$  takes the local minimum). (a)  $\alpha_p = 0.07\Delta_0$ . (b)  $\alpha_p = 0.04\Delta_0$ . (c)  $\alpha_p = 0.01\Delta_0$ . (d)  $\alpha_p = 0.001\Delta_0$ . The horizontal lines indicate the values ( $\Omega =$ )  $0.46\Delta_0$ ,  $0.69\Delta_0$ , and  $0.92\Delta_0$  from bottom to top.

TPA spectrum shows a peak is between  $E_g$  and  $\Delta$ .<sup>23</sup> This behavior is caused by a shift of the spectrum to a lower energy with increasing  $\alpha_p$ .

The THG intensities for various values of  $1/t_0^2$  are shown in Fig. 7. A small value of  $1/t_0^2$  corresponds to a small width of the incident pulse in the frequency space. The temperature at which the THG intensity shows a peak does not vary with  $1/t_0^2$ , but the peak becomes sharp with decreasing  $1/t_0^2$ . This behavior supports an expectation about the peak in the THG intensity suggested in Ref. 8.

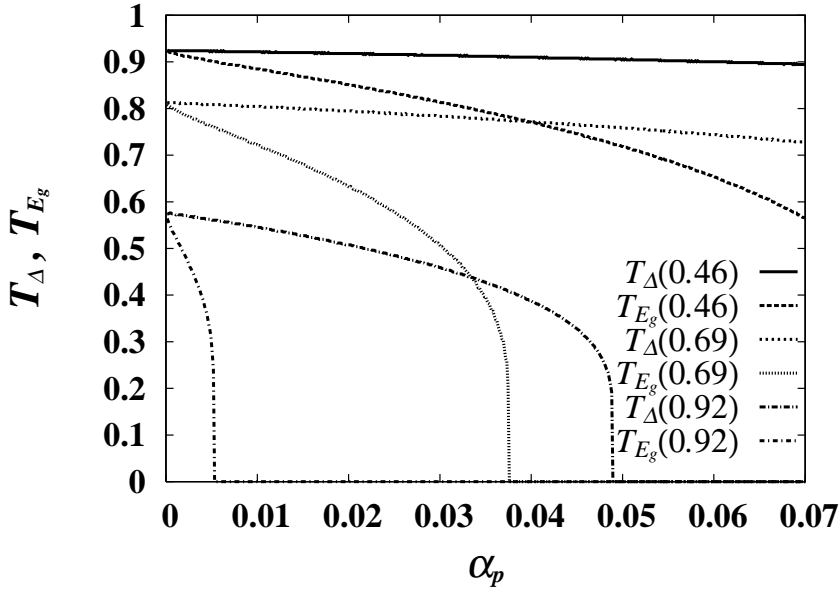


**Fig. 5.**  $T_{\Delta}$  ( $T_{E_g}$ ), which is the intersection of  $\Delta$  ( $E_g$ ) and  $\Omega$ . Numbers in parentheses are values of  $\Omega$ .  $T_{\Delta}$  and  $T_{E_g}$  are values of the temperature normalized by  $T_C$ .

### 3.3 Quantitative evaluation

The THG intensity divided by the incident pulse is approximately written as

$$\left| \frac{4\pi d}{2n_{3\Omega}c} \right|^2 \frac{|J_{3\Omega}|^2}{|E_{\Omega}|^2} = \left| \frac{4\pi d\sigma_0}{2n_{3\Omega}c} \right|^2 \left( \frac{e|\bar{E}_0|\xi_0}{\Delta_0} \right)^4 \left( \frac{l}{\xi_0} \right)^2 |j_{3\Omega}|^2$$

(see, for example, Ref. 24). Here,  $n_{3\Omega}$  is the refractive index,  $|n_{3\Omega}|^2 \simeq 4\pi|\sigma_{3\Omega}|/3\Omega$ , and  $d$  is the thickness of the film. When we set  $\xi_0 = 5$  nm,<sup>25</sup>  $\Delta_0 = 2.7$  meV,  $d = 24$  nm, and  $\sigma_0 = 1.5 \times 10^4 \Omega^{-1} \text{ cm}^{-1}$ , and assume  $|\sigma_{3\Omega}| \simeq \sigma_0$  because we consider the case of  $3\Omega > \Delta$ , we obtain

$$\left| \frac{4\pi d\sigma_0}{2n_{3\Omega}c} \right|^2 \left( \frac{e|\bar{E}_0|\xi_0}{\Delta_0} \right)^4 \left( \frac{l}{\xi_0} \right)^2 \simeq 1.37 \times 10^{-5}$$

for  $l = 0.8$  nm ( $l \simeq 0.58 \sim 0.83$  nm<sup>26</sup>),  $|\bar{E}_0| = 3.5$  kV/cm, and  $\Omega = 0.92\Delta_0$ . Then  $\left| \frac{4\pi d\sigma_0}{2n_{3\Omega}c} \right|^2 \left( \frac{e|\bar{E}_0|\xi_0}{\Delta_0} \right)^4 \left( \frac{l}{\xi_0} \right)^2 |j_{3\Omega}|^2 \simeq 6.85 \times 10^{-5}$  using the calculated results of  $|j_{3\Omega}|^2$  in Fig. 6(b) for  $\Omega = 0.92\Delta_0$ . This is about the same value as an experimental value in Ref. 8, where  $8 \times 10^{-5}$  was reported as a value of the THG intensity normalized by that of the pump pulse.

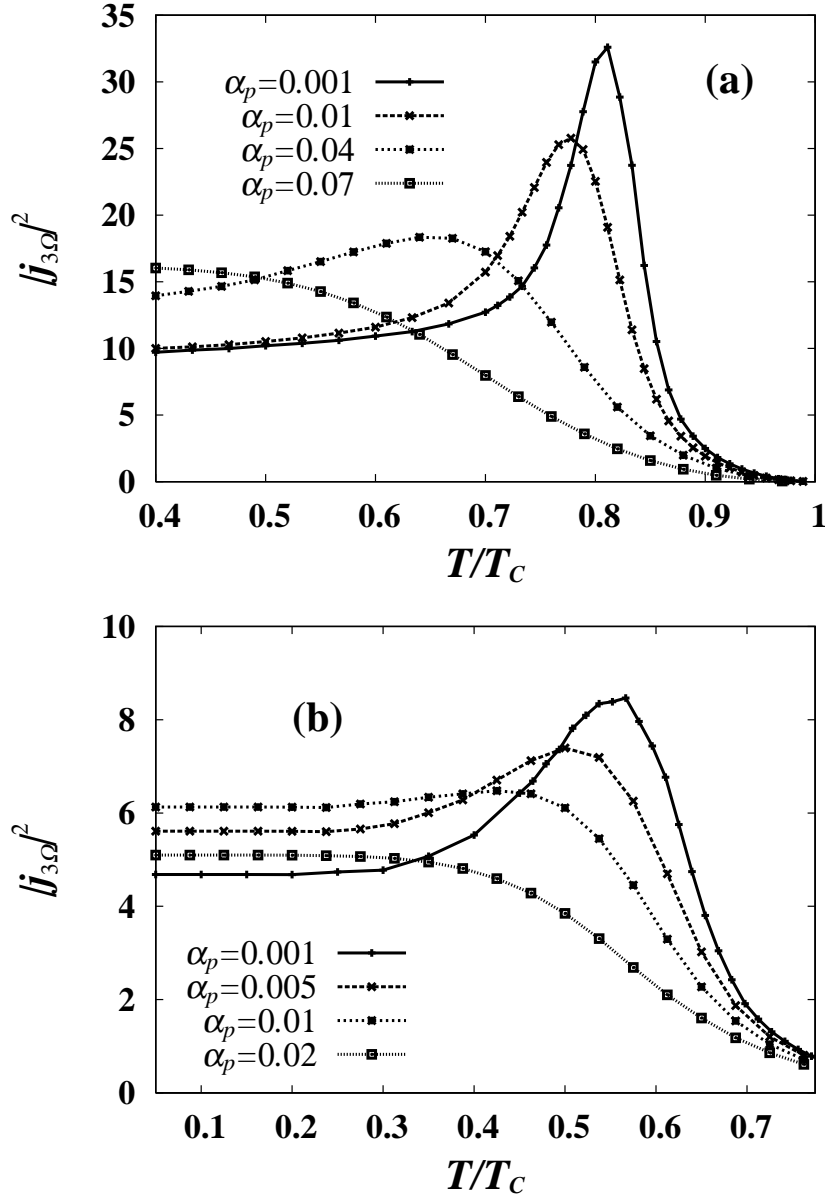


**Fig. 6.** Temperature dependences of the dimensionless THG intensity  $|j_{3\Omega}|^2$  for various values of  $\alpha_p$  with  $\Omega$  the frequency of the incident pulse. (a)  $\Omega = 0.69\Delta_0$  and (b)  $\Omega = 0.92\Delta_0$ .  $1/t_0^2 = 0.003\Delta_0^2$ .

#### 4. Diamagnetic Term

When we take account of the diamagnetic coupling in the interaction between electrons and external fields,<sup>27</sup> there is an additional term in a nonlinear current as follows:

$$J_\omega^d = \frac{-e^2}{m} \int \frac{d\omega'}{2\pi} A_{\omega'} \int_{\text{FS}} \frac{mk_F}{2\pi} \int \frac{d\epsilon}{4\pi i} \text{Tr} [\hat{\tau}_3 \hat{g}_{\epsilon+\omega-\omega',\epsilon}^K]. \quad (20)$$

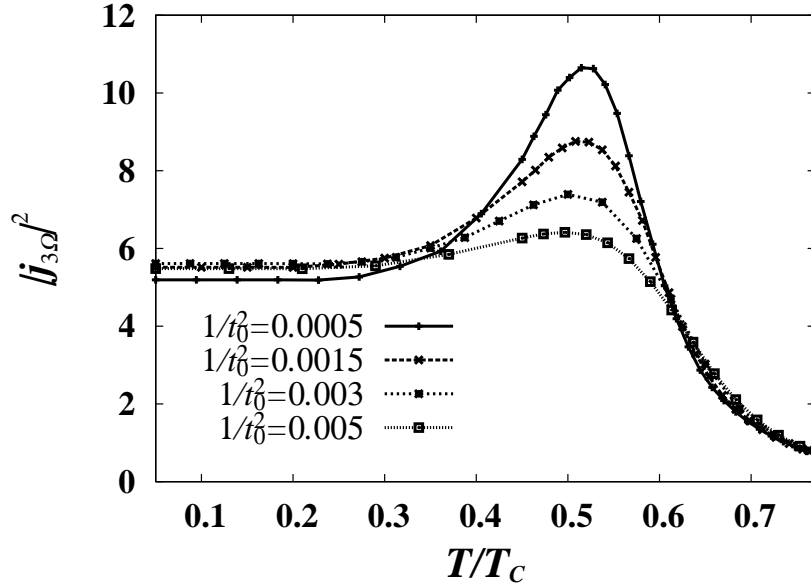


**Fig. 7.** Dependence of the dimensionless THG intensity on temperature for various values of  $1/t_0^2$  (with  $1/t_0$  proportional to the pulse width in the frequency space).  $\alpha_p = 0.005\Delta_0$  and  $\Omega = 0.92\Delta_0$ .

In this case, there are also additional terms in the kinetic equations. These are written as

$$\int \frac{d\omega_1 d\omega_2}{(2\pi)^2} \frac{e^2}{2} A_{\omega_1} A_{\omega_2} \frac{1}{m} [\hat{g}_\epsilon^+ - \hat{g}_{\epsilon'}^+] \delta(\epsilon - \epsilon' - \omega_1 - \omega_2) \quad (21)$$

and

$$\int \frac{d\omega_1 d\omega_2}{(2\pi)^2} \frac{e^2}{2} A_{\omega_1} A_{\omega_2} \frac{1}{m} (t_\epsilon^h - t_{\epsilon'}^h) [\hat{g}_\epsilon^+ - \hat{g}_{\epsilon'}^-] \delta(\epsilon - \epsilon' - \omega_1 - \omega_2) \quad (22)$$

for the left-hand sides of Eqs. (3) and (4), respectively. The additional term arises in the solution [Eq. (5)] and is written as<sup>28</sup>

$$g'_{\epsilon, \epsilon'} \hat{\tau}_3 + i f'_{\epsilon, \epsilon'} \hat{\tau}_2 \quad (23)$$

with  $i\hat{\tau}_2 = \begin{pmatrix} 0 & 1 \\ -1 & 0 \end{pmatrix}$ .

Since  $(g', f')$  are different matrix elements from  $(g, f)$  in Sects. 2 and 3, they can be obtained separately. The solution is written as

$$\begin{pmatrix} g'_{\epsilon, \epsilon'}{}^s \\ f'_{\epsilon, \epsilon'}{}^s \end{pmatrix} = \int \frac{d\omega_1 d\omega_2}{(2\pi)^2} \frac{e^2}{2} A_{\omega_1} A_{\omega_2} \delta(\epsilon - \epsilon' - \omega_1 - \omega_2) \frac{1}{m} \begin{pmatrix} \bar{g}'_{\epsilon, \epsilon'}{}^s \\ \bar{f}'_{\epsilon, \epsilon'}{}^s \end{pmatrix} \quad (24)$$

with

$$\begin{pmatrix} \bar{g}'_{\epsilon, \epsilon'}{}^\pm \\ \bar{f}'_{\epsilon, \epsilon'}{}^\pm \end{pmatrix} := \hat{M}'_{\epsilon, \epsilon'}{}^{\pm\pm} \begin{pmatrix} 1 \\ 0 \end{pmatrix} \quad (25)$$

and

$$\begin{pmatrix} \bar{g}'_{\epsilon,\epsilon'}(a) \\ \bar{f}'_{\epsilon,\epsilon'}(a) \end{pmatrix} := (t_\epsilon^h - t_{\epsilon'}^h) \hat{M}'_{\epsilon,\epsilon'}{}^{+-} \begin{pmatrix} 1 \\ 0 \end{pmatrix}. \quad (26)$$

Here,

$$\hat{M}'_{\epsilon,\epsilon'}{}^{ab} := \frac{i [\hat{\tau}_3 - X'_{\epsilon,\epsilon'}{}{}^{ab} \hat{\tau}_0 - Y'_{\epsilon,\epsilon'}{}{}^{ab} \hat{\tau}_1]}{z_\epsilon^a + z_{\epsilon'}^b + 2i\alpha_p X'_{\epsilon,\epsilon'}{}{}^{ab}}, \quad (27)$$

where  $X'_{\epsilon,\epsilon'}{}{}^{ab} := (\epsilon_p^a \epsilon_p^b - \Delta_\epsilon^a \Delta_{\epsilon'}^b) / z_\epsilon^a z_{\epsilon'}^b$  and  $Y'_{\epsilon,\epsilon'}{}{}^{ab} := (\epsilon_p^a \Delta_{\epsilon'}^b - \Delta_\epsilon^a \epsilon_p^b) / z_\epsilon^a z_{\epsilon'}^b$ . Using the above quantities, Eq. (20) is rewritten as

$$J_\omega^d = \frac{-1}{2} \left( \frac{e^2}{m} \right)^2 \int \frac{dwdw'}{(2\pi)^3} A_{\omega-2w} A_{w+w'/2} A_{w-w'/2} \frac{mk_F}{2\pi} \int \frac{d\epsilon}{4\pi i} \text{Tr} \left[ \hat{\tau}_3 \hat{g}'_{\epsilon+w,\epsilon-w}{}^K \right]. \quad (28)$$

By using the electric field introduced in Sect. 3, the nonlinear current is written as

$$J_\omega^d = \sigma_0 |E_\Omega| \left( \frac{e |\bar{E}_0| \xi_0}{\Delta_0} \right)^2 \left( \frac{\Delta_0}{E_F} \right)^2 \frac{9\pi^2 \xi_0}{8l} j_\omega^d. \quad (29)$$

Here,  $E_F = k_F^2 / 2m$  is the Fermi energy and

$$j_\omega^d = \frac{-1}{48} \int dwdw' t_0^2 \bar{A}_{\omega-2w} \bar{A}_{w+w'/2} \bar{A}_{w-w'/2} \int \frac{d\epsilon}{4\pi i} \text{Tr} \left[ \hat{\tau}_3 \hat{g}'_{\epsilon+w,\epsilon-w}{}^K \right]. \quad (30)$$

We consider the ratio  $|J_{3\Omega}^d|^2 / |J_{3\Omega}|^2$  in order to evaluate this term quantitatively. From Eqs. (18) and (29),

$$\frac{|J_{3\Omega}^d|^2}{|J_{3\Omega}|^2} = \left( \frac{\Delta_0}{E_F} \right)^4 \left( \frac{3\pi \xi_0}{2\sqrt{2}l} \right)^4 \frac{|j_{3\Omega}^d|^2}{|j_{3\Omega}|^2}. \quad (31)$$

Here,  $3\pi \xi_0 / 2\sqrt{2}l \simeq 20.8$  for  $\xi_0 = 5$  nm and  $l = 0.8$  nm, and then  $|J_{3\Omega}^d|^2 / |J_{3\Omega}|^2 \simeq 2 \times 10^{-3}$  when  $\Delta_0 / E_F = 0.01$  and  $|j_{3\Omega}^d|^2 / |j_{3\Omega}|^2 = 1$  (this last value is an overestimated value as mentioned below). Thus, the diamagnetic term is negligible as suggested in the annotation of Ref. 10 (Ref. 14 therein). This result is consistent with the experimental result that the diamagnetic term is not observed.<sup>12</sup>

The result of a numerical calculation shows that  $|j_{3\Omega}^d|^2 / |j_{3\Omega}|^2$  is smaller than 1. The reason for this is that there is no increase due to the amplitude mode in  $|j_{3\Omega}^d|^2$ . The absence of the amplitude mode in  $|j_{3\Omega}^d|^2$  is the result of the properties of the diamagnetic coupling term, which is represented by  $\hat{\tau}_3$  and  $i\hat{\tau}_2$  in Eq. (23). ( $\hat{\tau}_3$  and  $i\hat{\tau}_2$  indicate the density fluctuation and the phase mode, respectively. The amplitude mode in Sect. 2 comes from  $\hat{\tau}_1$ .)

## 5. Summary and Discussion

In this paper a theoretical study of the third-harmonic generation in dirty BCS superconductors was carried out. We calculated the temperature dependence and frequency dependence of the THG intensity, and showed that the vertex correction term including the amplitude mode is dominant. We introduced the effect of paramagnetic impurities, and showed that time-reversal symmetry breaking destabilizes the amplitude mode and that this effect is reflected in the THG intensity.

We showed that the dependences of the THG intensity on temperature and pulse width reproduce experimental results at the limit where the effect of paramagnetic impurities is small. Quantitatively, almost the same result as the experimental result was obtained. In addition, it is known that the diamagnetic term is small in the experiment.<sup>12</sup> The calculated result of Sect. 4 gives an explanation of this. This result is based on the fact that the reduction effect due to the superconducting gap being smaller than the Fermi energy is more dominant than the increase caused by the mean free path being shorter than the coherence length.

It is known that the effect of time-reversal symmetry breaking (due to paramagnetic impurities in this paper) can also be obtained by applying an in-plane magnetic field.<sup>29</sup> Referring to Figs. 2(a) and 2(b), the dependence of the THG intensity on  $\alpha_p$  differs between the term including the amplitude mode and that not including this mode. Therefore, the results of our calculation show that the presence of the amplitude mode can be confirmed experimentally by applying a magnetic field in the plane.

## Acknowledgement

The numerical computation in this work was carried out at the Yukawa Institute Computer Facility.

## References

- 1) C. Giannetti, M. Capone, D. Fausti, M. Fabrizio, F. Parmigiani, and D. Mihailovic, *Adv. Phys.* **65**, 58 (2016).
- 2) A. Schmid, *Phys. Kondens. Mater.* **8**, 129 (1968).
- 3) A. F. Volkov and S. M. Kogan, *Sov. Phys. JETP* **38**, 1018 (1974).
- 4) P. W. Anderson, *Phys. Rev.* **112**, 1900 (1958).
- 5) R. Sooryakumar and M. V. Klein, *Phys. Rev. Lett.* **45**, 660 (1980).
- 6) P. B. Littlewood and C. M. Varma, *Phys. Rev. B* **26**, 4883 (1982).
- 7) R. Matsunaga, Y. I. Hamada, K. Makise, Y. Uzawa, H. Terai, Z. Wang, and R. Shimano, *Phys. Rev. Lett.* **111**, 057002 (2013).
- 8) R. Matsunaga, N. Tsuji, H. Fujita, A. Sugioka, K. Makise, Y. Uzawa, H. Terai, Z. Wang, H. Aoki, and R. Shimano, *Science* **345**, 1145 (2014).
- 9) In Ref. 8, a theoretical work<sup>30</sup> is cited as an explanation of the amplitude mode in the THG intensity. In this theory, however, the paramagnetic coupling term<sup>27</sup> is not included because this calculation takes the clean and local limit. The linear absorption spectrum in the experiment<sup>8</sup> indicates that this coupling term is effective because there is a clear gap structure in the spectrum. Thus, the paramagnetic coupling term cannot be neglected in calculations of response functions,<sup>10</sup> and it makes a predominant contribution to the THG intensity as shown in Sect. 3.
- 10) T. Jujo, *J. Phys. Soc. Jpn.* **84**, 114711 (2015).
- 11) B. I. Ivlev, *JETP Lett.* **15**, 313 (1972).
- 12) R. Matsunaga, N. Tsuji, K. Makise, H. Terai, H. Aoki, and R. Shimano, *Phys. Rev. B* **96**, 020505(R) (2017).
- 13) G. M. Éliashberg, *Zh. Eksp. Teor. Fiz.* **61**, 1254 (1971) [*Sov. Phys. JETP* **34**, 668 (1972)].
- 14) L. V. Keldysh, *Sov. Phys. JETP* **20**, 1018 (1965).
- 15) K. D. Usadel, *Phys. Rev. Lett.* **25**, 507 (1970).
- 16) N. B. Kopnin, *Theory of Nonequilibrium Superconductivity* (Oxford University Press, New York, 2001), Chaps. 5 and 9.
- 17) A. A. Abrikosov and L. P. Gor'kov, *Sov. Phys. JETP* **8**, 1090 (1959).
- 18) A. A. Abrikosov and L. P. Gor'kov, *Sov. Phys. JETP* **12**, 1243 (1961).



- 19) S. Skalski, O. Betbeder-Matibet, and P. R. Weiss, Phys. Rev. **136**, A1500 (1964).
- 20) P. W. Anderson, J. Phys. Chem. Solids **11**, 26 (1959).
- 21) D. Vollhardt and P. Wölfle, Phys. Rev. B **22**, 4666 (1980).
- 22) T. Jujo, J. Phys. Soc. Jpn. **86**, 024709 (2017).
- 23) T. Jujo, presented at LT28, 28th Int. Conf. on Low Temperature Physics, 2017.
- 24) Y. R. Shen, *The Principles of Nonlinear Optics* (Wiley, New Jersey, 2003) Chap. 7.
- 25) Y. Ikebe, R. Shimano, M. Ikeda, T. Fukumura, and M. Kawasaki, Phys. Rev. B **79**, 174525 (2009).
- 26) A. Semenov, B. Günther, U. Böttger, H.-W. Hübers, H. Bartolf, A. Engel, A. Schilling, K. Ilin, M. Siegel, R. Schneider, D. Gerthsen, and N. A. Gippius, Phys. Rev. B **80**, 054510 (2009).
- 27) Terms such as the paramagnetic coupling and the diamagnetic coupling between electrons and electromagnetic fields are the same as those in Ref. 31.
- 28) It is known that only the anisotropic term remains in the diamagnetic term.<sup>32</sup> The value of the anisotropic term with vertex corrections included is at most several times the value of the isotropic term without vertex corrections. Thus, it is sufficient to evaluate the latter case in order to find out whether the diamagnetic term or the paramagnetic term dominates.
- 29) K. Maki, in *Superconductivity*, ed. R. D. Parks (Dekker, New York, 1969) Chap. 18.
- 30) N. Tsuji and H. Aoki, Phys. Rev. B **92**, 064508 (2015).
- 31) J. R. Schrieffer, *Theory of Superconductivity* (Addison-Wesley, Redwood City, CA, 1983) revised ed., Chap. 8.
- 32) A. A. Abrikosov and V. M. Genkin, Sov. Phys. JETP **38**, 417 (1974).